AWARD NUMBER: W81XWH-15-1-0111

TITLE: Drosophila as a Screening Platform for Novel Lung Cancer Therapeutics

PRINCIPAL INVESTIGATOR: Ross L. Cagan

CONTRACTING ORGANIZATION: Icahn School of Medicine at Mount Sinai
New York, NY 10029

REPORT DATE: September 2016

TYPE OF REPORT: Annual

PREPARED FOR: U.S. Army Medical Research and Materiel Command
Fort Detrick, Maryland 21702-5012

REPORT DOCUMENTATION PAGE

Form Approved
OMB No. 0704-0188

1. REPORT DATE	**2. REPORT TYPE**	**3. DATES COVERED**
September 2016	Annual	1 Sep 2015 - 31 Aug 2016

4. TITLE AND SUBTITLE
Drosophila as a Screening Platform for Novel Lung Cancer Therapeutics

5a. CONTRACT NUMBER

5b. GRANT NUMBER
W81XWH-15-1-0111

5c. PROGRAM ELEMENT NUMBER

6. AUTHOR(S)

Ross L. Cagan

ross.cagan@mssm.edu

5d. PROJECT NUMBER

5e. TASK NUMBER

5f. WORK UNIT NUMBER

7. PERFORMING ORGANIZATION NAME(S) AND ADDRESS(ES)
Icahn School of Medicine at Mount Sinai
New York, NY 10029

8. PERFORMING ORGANIZATION REPORT NUMBER

9. SPONSORING / MONITORING AGENCY NAME(S) AND ADDRESS(ES)
U.S. Army Medical Research and Materiel Command
Fort Detrick, Maryland 21702-5012

10. SPONSOR/MONITOR'S ACRONYM(S)

11. SPONSOR/MONITOR'S REPORT NUMBER(S)

12. DISTRIBUTION / AVAILABILITY STATEMENT
Approved for Public Release; Distribution Unlimited

13. SUPPLEMENTARY NOTES

14. ABSTRACT
The research in this grant is designed to explore the effects of genetic and genomic complexity in lung cancer progression and response to therapeutics. Using Drosophila, we are establishing a set of 'personalized fly lines', each which represents a separate patient. In this Progress Report, I discuss our initial studies in building these lines. In addition, I discuss our results with screening a library of 1200 FDA approved drugs. We provide evidence that a two drug cocktail, trametinib plus fluvastatin, synergize to improve efficacy and minimize toxicity in fly and human cell line models.

15. SUBJECT TERMS-

16. SECURITY CLASSIFICATION OF:			**17. LIMITATION OF ABSTRACT**	**18. NUMBER OF PAGES**	**19a. NAME OF RESPONSIBLE PERSON**
a. REPORT	**b. ABSTRACT**	**c. THIS PAGE**			USAMRMC
U	U	U	UU		**19b. TELEPHONE NUMBER** *(include area code)*

Table of Contents

INTRODUCTION

The research in this grant is designed to explore the effects of genetic and genomic complexity in lung cancer progression and response to therapeutics. Using Drosophila, we are establishing a set of 'personalized fly lines', each which represents a separate patient. In this Progress Report, I discuss our initial studies in building these lines. In addition, I discuss our results with screening a library of 1200 FDA approved drugs. We provide evidence that a two drug cocktail, trametinib plus fluvastatin, synergize to improve efficacy and minimize toxicity in fly and human cell line models.

KEYWORDS:

Drosophila, lung adenocarcinoma, trametinib, fluvastatin

Progress Report for LCRP grant W81XWH-15-1-0111

Drosophila as a Screening Platform for Novel Lung Cancer Therapeutics

Accomplishments

What were the major goals of the project?

This proposal uses Drosophila to explore how tumor complexity—common plus rare variants—affect tumor progression. To address this issue, I proposed to build 15 fly models, each modeling a different patient or commonly used cell line. These fly lines will be used to explore tumor complexity including response to drugs.

Two Specific Aims were proposed:

Specific Aim 1: Assess functional relevance of rare variants. Using sequencing data from patients and from cell lines, we will pair five 'base avatars' with 15 newly constructed 'complex avatars' designed to mimic the patient's mutation load at two levels of complexity. 'Base' vs. 'complex' avatars will be compared for tumor progression by quantitating eight phenotypic and biochemical assays.

Specific Aim 2: Examine drug response in Drosophila lung cancer models. As a step towards understanding the role of rare variants in drug response, we will screen each avatar with a broad set of 1200 FDA approved drugs. Multiple rounds of screening will be used to identify drug cocktails. We will then compare efficacy of drugs that are optimal for each 'base avatar' with their activity against the paired 'complex avatar'.

What was accomplished under these goals?

Specific Aim #1. Here I propose to develop a set of 'base' (genetically simple) and 'complex (more extensively multigenic) fly models to match specific patients. Since writing the Proposal, the TCGA data has been updated. To reflect this updated information, we re-analyzed EGFR-class patients (EGFR, ERBB2, ERBB4) to include copy number variation and to capture newly included patients. We took advantage of advanced analysis now available within the Sloan-Kettering 'CBioportal' which assessed each variant to determine its likely impact on protein function. Table 1 shows the updated analysis, translated to specific fly lines.

We are currently assembling these fly lines, and have completed lines for the first three listed in Table 1.

	patient#	*oncogenes* *tumor suppressors*
1	*base*	*EGFR*
2	*E5b*	*EGFR* *P53*
3	*4080/2708b*	*EGFR* *P53 PTEN*
4	*2722b*	*EGFR HTL* *P53*
5	*2787*	*EGFR* *P53 CDK1 KUG/FAT*
6	*2708*	*EGFR SCRO MYC FKH* *P53 PTEN*
7	*3789*	*EGFR CDK4 RAC1* *P53*
8	*2698*	*EGFR CycD CycE* *P53 AGO VAP MSH6*
9	*4593*	*EGFR CycD CycE* *P53 AGO LAR*
10	*1081*	*EGFR HTL* *P53 PTEN*
11	*2722*	*EGFR HTL* *P53 AGO*

Table 1. Fly avatars.

All of the remaining lines are under construction and I anticipate stable Drosophila lines will be established by the end of the calendar year.

Specific Aim #2: In this Aim, I proposed to screen a library of 1200 FDA-approved drugs for the ability to 'rescue' our fly lung cancer lines. While assembling the personalized fly models, we embarked on this screen against a 'base' Ras model and a Ras/PTEN model (Levine and Cagan, 2016). As described in the original proposal, transgenes were targeted to the developing fly trachea using the *btl-GAL4* driver, yielding *btl>Ras* and *btl>Ras/PTEN flies.* As shown in Figure 1, the result was enlargement of trachea including tracheal branches (*from* Levine and Cagan, 2016). We then established and calibrated a 'rescue from lethality' assay.

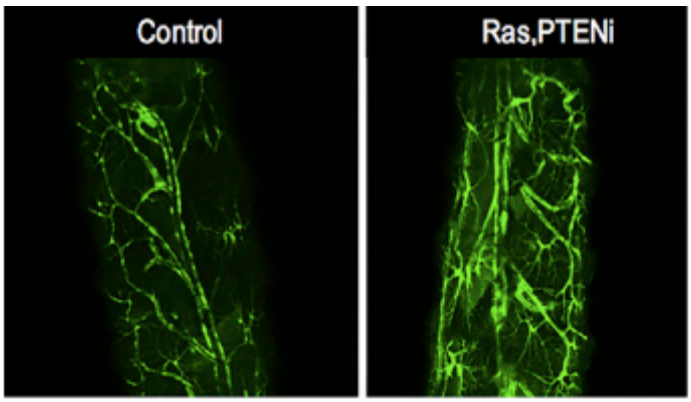

Figure 1. *btl>Ras/PTEN* animals displayed enlarged trachea.

Screening the full FDA library yielded eight 'hits', shown in Figure 2. These hits included chemotherapy-related drugs as well as two targeted drugs, trametinib and fluvastatin. Trametinib is an inhibitor of MEK, a downstream target of EGFR and Ras. Fluvastatin is a statin-class drug that inhibits HMG-CoA reductase. Our data indicated that at least part of fluvastatin's activity is through its ability to suppress the cholesterol modification required to target the Ras protein to the surface.

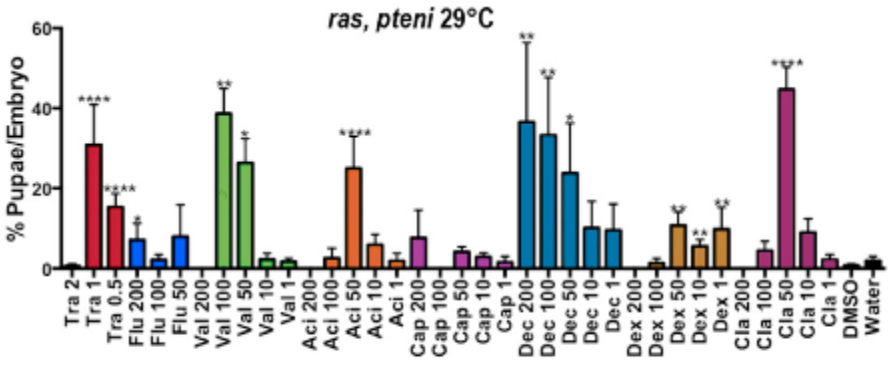

Figure 2. Eight positive 'hits' rescued *btl>Ras/PTEN* animals to pupariation. Drug concentrations are mM. Aci, aciclovir; Cap, capecitabine; Cla, cladribine; Dec, decitabine; Dex, dexrazoxane; Flu, fluvastatin; Tra, trametinib; Val, valaciclovir. (*p%0.05, ** p%0.01, *** p % 0.01, and **** p % 0.0001). From *Levine and Cagan, 2016.*

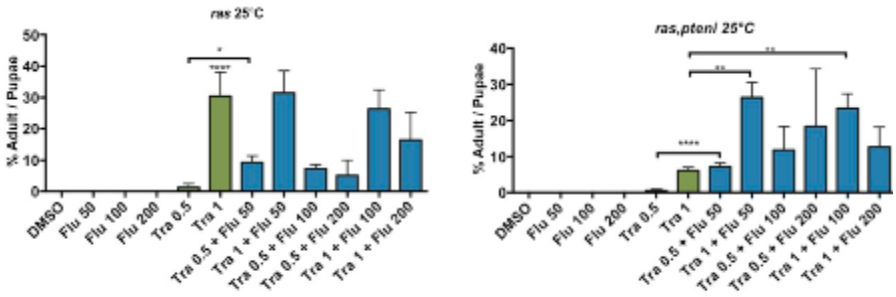

Figure 3. 50 μM fluvastatin + 0.5 mM trametinib showed better rescue to adulthood than 0.5 mM trametinib alone (p=0.05). From Levine and Cagan, 2016.

A key hypothesis of the Grant is that drug combinations may prove more useful than single targeted therapies. This proved to be the case in some instances. In particular, trametinib plus fluvastastin proved better able to rescue *btl>Ras/PTEN* flies to adulthood, as shown in Figure 3. The synergistic rescue was observed for *btl>Ras/PTEN* but not for *btl>Ras* alone, emphasizing the changing response to drugs as tumors increase in complexity.

Finally, we were able to validate this drug combination in an A549 lung cancer cell line (Figure 4). As we develop the EGFR-based fly avatars, we will be testing these initial hits to determine how useful they are in suppressing the transformation phenotypes observed in the fly avatar lines.

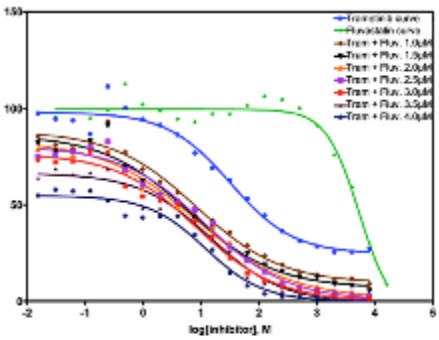

Figure 4. Percent viability of A549 cells determined by MTT assay plotted on a logarithmic molar dose curve scale. Based on Chou-Talalay CI index, 1-3 μM fluvastatin synergistically lowered the IC50 of trametinib. From Levine and Cagan, 2016.

What opportunities for training and professional development has the project provided?

Through weekly meetings and journal clubs, this Project provided scientific mentorship. In addition, I meet with each member of the Project one-on-one every other week to provide more extensive mentorship on both the science and regarding careers decisions.

How were the results disseminated to communities of interest?

I have given approximately 15 external, invited talks in the past year to discuss our approach using screening of multigenic cancer models. In addition, we recently published a paper reporting our initial characterization and drug screening of a Drosophila lung cancer model:

Levine B and Cagan R. (2016). Drosophila Lung Cancer Models Identify Trametinib Plus A Statin as a Candidate Therapeutic. Cell Reports, doi: 10.1016/j.celrep.2015.12.105.

What do you plan to do during the next reporting period to accomplish the goals?

I anticipate that we will complete assembly of the complex, personalized fly models and that screening will commence to identify useful drug cocktails for each model.

Impact

What was the impact on the development of the principal discipline(s) of the project?

Cancer remains a key challenge to our healthcare system. Our initial results emphasize the utility of screening in an unbiased fashion, and the potential utility of drug cocktails in addressing tumor complexity.

What was the impact on other disciplines?
Nothing to Report.

What was the impact on technology transfer?
Nothing to Report.

What was the impact on society beyond science and technology?
Nothing to Report.

CHANGES/PROBLEMS:

Changes in approach and reasons for change
No significant changes were made in the approach or scope.

Actual or anticipated problems or delays and actions or plans to resolve them
We faced some challenges in building the highly complex transgenes for knockdown. After some technology development, we have settled on a ‘stitching’ method in which PCR products are quickly assembled into a single knockdown construct.

Changes that had a significant impact on expenditures
Nothing to Report.

Significant changes in use or care of human subjects, vertebrate animals, biohazards, and/or select agents
Nothing to Report.

Significant changes in use or care of human subjects
Nothing to Report.

Significant changes in use or care of vertebrate animals.
Nothing to Report.

Significant changes in use of biohazards and/or select agents
Nothing to Report.

PRODUCTS

One journal publication:

Levine B and Cagan R. (2016). Drosophila Lung Cancer Models Identify Trametinib Plus A Statin as a Candidate Therapeutic. Cell Reports, doi: 10.1016/j.celrep.2015.12.105.

Website(s) or other Internet site(s)

Nothing to Report.

Technologies or techniques

Nothing to Report.

Inventions, patent applications, and/or licenses

Nothing to Report.

Other Products

Nothing to Report.

PARTICIPANTS & OTHER COLLABORATING ORGANIZATIONS

- ***Provide the following information for: (1) PDs/PIs; and (2) each person who has worked at least one person month per year on the project during the reporting period, regardless of the source of compensation (a person month equals approximately 160 hours of effort). If information is unchanged from a previous submission, provide the name only and indicate "no change."***

What individuals have worked on the project?
Ross Cagan, no change

Name:	*Ross Cagan*
Project Role:	*PI*
Researcher Identifier (e.g. ORCID ID):	
Nearest person month worked:	*2.4*
Contribution to Project:	*Dr. Cagan provided overall project guidance.*
Funding Support:	*NA*

Name:	*Masahiro Sonoshita*
Project Role:	*Postdoctoral fellow*
Researcher Identifier (e.g. ORCID ID):	
Nearest person month worked:	*8*
Contribution to Project:	*Dr. Sonoshita has taken the lead in the project, working with Dr. Das to develop the transgenic animals.*
Funding Support:	*NA*

Name:	*Alexander Teague*
Project Role:	*Senior Associate Researcher*
Researcher Identifier (e.g. ORCID ID):	

Nearest person month worked:	*8*
Contribution to Project:	*Mr. Teague has provided overall technical support including animal care.*
Funding Support:	*NA*

Name:	*Tirtha Das*
Project Role:	*Associate scientist*
Researcher Identifier (e.g. ORCID ID):	
Nearest person month worked:	*4*
Contribution to Project:	*Dr. Das worked with Dr. Sonoshita to develop the required transgenic animals.*
Funding Support:	*NA*

Name:	*Erdem Bangi*
Project Role:	*Senior scientist*
Researcher Identifier (e.g. ORCID ID):	
Nearest person month worked:	*2*
Contribution to Project:	*Dr. Bangi provided the initial genomics analysis of lung cancer patients.*
Funding Support:	*NA*

Has there been a change in the active other support of the PD/PI(s) or senior/key personnel since the last reporting period?

The following were listed as “Active” but have now ended:

NIH R01 EY11495
Programmed cell death in the *Drosophila* eye
Role: PI. Expired 7-31-15

NIH R01 CA170495
A Drosophila Model Linking Diet-induced Obesity and Cancer (PQ1)
Role: PI. Expired 6-30-16.

ACS RSGM-11-018-01CDD
A Novel Class of Therapeutic Kinase Inhibitors for Treatment of Men2
Role: PI. Expired 12-31-15

The following grants are currently active:

W81XWH-15-1-0111 09/01/2015 – 08/31/2017 2.4 calendar
Dept. of Defense LCRP Idea Award $175,000
Drosophila as a Screening Platform for Novel Lung Cancer Therapeutics
Builds complex Drosophila models to explore role of rare variants.
Role: PI

U54OD020353-01 (Cagan) 08/01/2015-06/30/2020 3.6 calendar
NIH $305,593
A New Disease Platform Leveraging Complex Drosophila and Mammalian Models
Builds a therapeutic platform, Drosophila-to-mammals
Role: PI

R01HL071207 (Gelb) 08/01/02-01/31/18 0.7 calendar
Molecular basis of Noonan syndrome and related disorder $275,177
Discover additional RASopathy genes and to seek therapies that reverse the hypertrophic cardiomyopathy associated with these disorders.
Role: Investigator

Rainwater Foundation 01/01/16-12/31/16 0.7 calendar
A Drosophila Approach towards a Novel Alzheimer's Therapeutics $153,724
Explores Drosophila as a platform for developing therapies for tauopathies.
Role: Co-Principal Investigator (Goate and Cagan)

018.16 09/01/16-08/31/16 0.7 calendar
Mary Kay Ash Foundation $100,000
Drosophila Models of Triple Negative Breast Cancer as a Platform To Identify Novel Therapeutics
Uses personalized fly TNBC models to identify candidate therapeutics
Role: PI

1P30CA196521-01 (Burakoff) 07/01/2015 - 06/30/2020 0.6 calendar
NIH/NCI $1,000,000
The Tisch Cancer Institute - Cancer Center Support Grant
Role: Co-Program Leader

What other organizations were involved as partners?
Nothing to report.

SPECIAL REPORTING REQUIREMENTS

Nothing to report.

APPENDICES

One manuscript is appended.

Article

Cell Reports

Drosophila Lung Cancer Models Identify Trametinib plus Statin as Candidate Therapeutic

Graphical Abstract

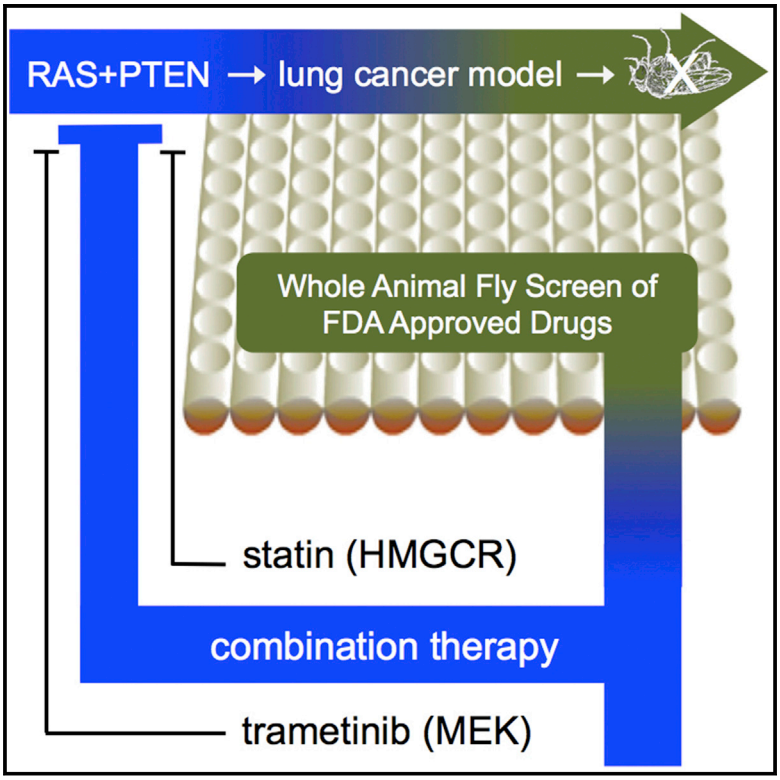

Authors

Benjamin D. Levine, Ross L. Cagan

Correspondence

ross.cagan@mssm.edu

In Brief

Levine and Cagan describe an oncogenic Ras-driven lung cancer model in *Drosophila* that is used in a whole-animal drug screen of over 1,000 FDA-approved compounds. Two hits, the MEK inhibitor trametinib and the statin fluvastatin, synergized to rescue oncogenic phenotypes and lethality.

Highlights

- A *Drosophila* Ras-Pten lung cancer model was established
- Altering cancer genes in the trachea led to growth and migration defects
- Screening identified trametinib plus fluvastatin as a candidate therapeutic cocktail
- Trametinib/fluvastatin showed synergistic efficacy in human lung cancer cell line

Levine & Cagan, 2016, Cell Reports *14*, 1–11
February 16, 2016
http://dx.doi.org/10.1016/j.celrep.2015.12.105

CellPress

Please cite this article in press as: Levine and Cagan, *Drosophila* Lung Cancer Models Identify Trametinib plus Statin as Candidate Therapeutic, Cell Reports (2016), http://dx.doi.org/10.1016/j.celrep.2015.12.105

Cell Reports
Article

Drosophila Lung Cancer Models Identify Trametinib plus Statin as Candidate Therapeutic

Benjamin D. Levine[1] and Ross L. Cagan[1,*]
[1]Department of Developmental and Regenerative Biology and the Graduate School of Biomedical Sciences, Icahn School of Medicine at Mount Sinai, One Gustave Levy Place, New York, NY 10029-1020, USA
*Correspondence: ross.cagan@mssm.edu
http://dx.doi.org/10.1016/j.celrep.2015.12.105

SUMMARY

We have developed a *Drosophila* lung cancer model by targeting Ras1^{G12V}—alone or in combination with PTEN knockdown—to the *Drosophila* tracheal system. This led to overproliferation of tracheal tissue, formation of tumor-like growths, and animal lethality. Screening a library of FDA-approved drugs identified several that improved overall animal survival. We explored two hits: the MEK inhibitor trametinib and the HMG-CoA reductase inhibitor fluvastatin. Oral administration of these drugs inhibited Ras and PI3K pathway activity, respectively; in addition, fluvastatin inhibited protein prenylation downstream of HMG-CoA reductase to promote survival. Combining drugs led to synergistic suppression of tumor formation and rescue lethality; similar synergy was observed in human A549 lung adenocarcinoma cells. Notably, fluvastatin acted both within transformed cells and also to reduce whole-body trametinib toxicity in flies. Our work supports and provides further context for exploring the potential of combining statins with MAPK inhibitors such as trametinib to improve overall therapeutic index.

INTRODUCTION

Lung cancer is the leading cause of cancer-related mortality worldwide, with non-small-cell lung cancer (NSCLC) accounting for 85% of disease diagnoses. Standard of care commonly includes a targeted therapy combined with chemoradiotherapy; multiple targeted therapies are currently approved for use in NSCLC. These drugs provide important first- and second-line therapies. In many patients, however, these drugs have shown limited success in suppressing tumor progression due to limited efficacy, emergent resistance, and significant toxicity. As a result, NSCLC continues to represent a significant unmet clinical need. Current efforts to identify new drugs and drug cocktails would benefit from whole-animal approaches that account for complex and often unpredictable drug activities. Here, we present a *Drosophila* model of lung cancer as a platform to identify and explore candidate therapeutics.

A number of publications have highlighted the similarities between *Drosophila* tracheal and vertebrate lung development (Roeder et al., 2012; Behr, 2010; Andrew and Ewald, 2010). The *Drosophila* tracheal system is an extensively branched tubular network that supplies oxygen to the fly. Both vertebrate lung and *Drosophila* tracheal systems are formed from an interconnected tubular hierarchy that begins in large primary tubes and branches into diminishing diameter segments that end in terminal branches. During *Drosophila* tracheal development, the branching process is highly dependent on fibroblast growth factor (FGF) signaling. Tracheal cells express the FGF receptor homolog Breathless (Btl), which responds to localized presence of the FGF ligand Branchless to initiate branching. Vertebrate lung development relies on FGF signaling in a similar manner during airway branching (Park et al., 1998; Bellusci et al., 1997).

Here, we present the results of tracheal-targeted expression of the oncogenic isoform Ras1^{G12V} plus knockdown of the PI3K-negative regulator PTEN. Activated Ras isoforms represent the most-common genetic mutations associated with NSCLC and are typically associated with activated PI3K pathway signaling (Kandoth et al., 2013; Cancer Genome Atlas Research Network, 2012). Screening a library of FDA-approved compounds yielded multiple hits, including the MEK inhibitor trametinib and the HMG-CoA reductase inhibitor fluvastatin. We provide evidence that these two drugs act synergistically to reduce the effects of Ras/PI3K pathway activation. The result is improved tracheal development, reduced overproliferation, and reduced whole-animal toxicity; the two drugs also acted synergistically to suppress growth in a standard human lung cancer cell line. We demonstrate that fluvastatin acts through multiple targets to improve overall efficacy, and our data suggest that fluvastatin may prove useful to reduce the whole-body toxicity profiles that are common to targeted therapies.

RESULTS

Drosophila Lung Cancer Model

To reliably manipulate gene sets, we built vectors containing multiple UAS elements using a "repeat ligation method" (Figure 1A; see Experimental Procedures). With this reiterative cloning approach, we created *Drosophila* lines with transgenes inserted into the same attP insertion site to ensure comparable expression levels. The resulting lines expressed transgenes that directed

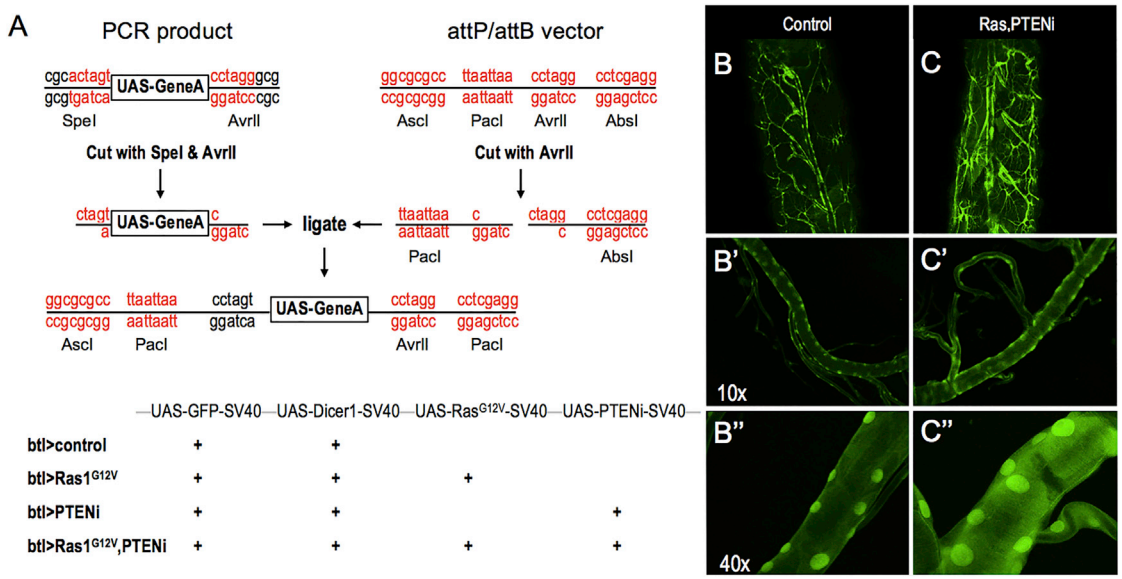

Figure 1. A Multigenic *Drosophila* Lung Cancer Model

(A) Multiple UAS-containing transgenes were combined into vectors using a repeat ligation method. Up to four UAS elements were added to a single vector in the order and orientation shown. The four transgenic lines used in this study are indicated in the lower panel.

(B–C'') *btl* > *Ras1*,*PTENi* larvae exhibited enlarged and thickened tracheal tubes compared to *btl* > *control* larvae. Higher magnification views are shown to visualize the enlarged nuclei.

expression of the oncogenic Ras1 isoform $Ras1^{G12V}$ and/or RNAi-mediated knockdown of the PI3K pathway inhibitor PTEN (*PTENi*), addressing two pathways commonly activated in NSCLC patients (Kandoth et al., 2013; Cancer Genome Atlas Research Network, 2012). To express these transgenes within the *Drosophila* trachea, we added the driver *breathless-gal4* (*btl-GAL4*) by standard genetic crosses. *btl-Gal4* is expressed primarily in the trachea; expression is also reported in midline glia within the ventral nerve cord (Shiga et al., 1996). The result was establishment of four lines: *btl* > *control*; *btl* > *Ras1*; *btl* > *PTENi*; and *btl* > *Ras1*,*PTENi*. The full genotypes are listed in Figure 1A; all include expression of the visible marker GFP to visualize transformed cells.

The transgenic line *btl* > *control* directed GFP expression primarily within tracheal tissue throughout development including the L3 larval stage, confirming specificity of the driver (Figure 1B). *btl* > *Ras1*,*PTENi* L3 larvae exhibited tracheal tubes with thicker walls than control animals, likely due to a significant increase in nuclear size typical of transformed cells (Figures 1C and S1). In addition, *btl* > *Ras1*,*PTENi* L3 larval tracheal tubes tended toward increased width (not significant; Figure S1) and exhibited fine terminal branching (Figure 1C). The result was a lethal phenotype: at 25°C, *btl* > *Ras1* and *btl* > *Ras1*, *PTENi* survived to pharate (late pupal) stage but exhibited low levels of eclosion to adulthood. At 29°C—a temperature at which the *btl-GAL4* driver is more active—both lines died during early larval (L1–L2) stages; *btl* > *PTENi*—lacking $Ras1^{G12V}$—showed no detectable phenotype (data not shown). Whereas we anticipate that lethality is due to tracheal expression, we cannot rule out a contribution by *btl-GAL4*'s midline expression.

Screen for Candidate Therapeutics

btl > *Ras1*,*PTENi* animals die as larvae at 29°C. Using a robotics-based screening approach and a 96-well format (see Experimental Procedures), we screened a library of 1,192 FDA-approved drugs for those that rescued animals to pupariation (Figure 2A). Hits were subsequently tested in *btl* > *Ras1* flies. Drugs were fed orally mixed in the animals' food, the screen was performed in duplicate, and potential hits were confirmed in a larger-scale format.

Eight hits were identified from this screen (Figure 2B). Interestingly, five of the hits are DNA analogs, three of which are used as chemotherapeutics including capecitabine (5-fluorouracil prodrug), decitabine (cytidine analog used to treat acute myeloid leukemia), and cladribine (purine analog used to treat hairy cell leukemia). The remaining two DNA analogs were aciclovir and its prodrug valaciclovir, which are guanosine analog antiviral drugs. The antioxidant dexrazoxane was also a weak hit. These provide validation that clinic-relevant hits can be identified in our screening setup.

Two pathway inhibitor drugs were identified. The targeted cancer therapeutic trametinib is a highly specific MEK inhibitor approved for metastatic melanoma. Fluvastatin is an HMG-CoA reductase inhibitor from the cholesterol-lowering statin family. Oral administration of trametinib at 1 μM significantly rescued *btl* > *Ras1* and *btl* > *Ras1*,*PTENi* pupal lethality at 25°C (Figures 2C and 2D) and larval lethality at 29°C (Figures 2E and 2F). Fifty micromolar fluvastatin directed a mild rescue of larval lethality in both genotypes (Figures 2E and 2F) but was ineffective in the more-stringent pupal lethality assay (Figures 2C and 2D). Along with radiation therapy, targeted therapies as stand-alone or adjuvant can yield positive outcomes in lung

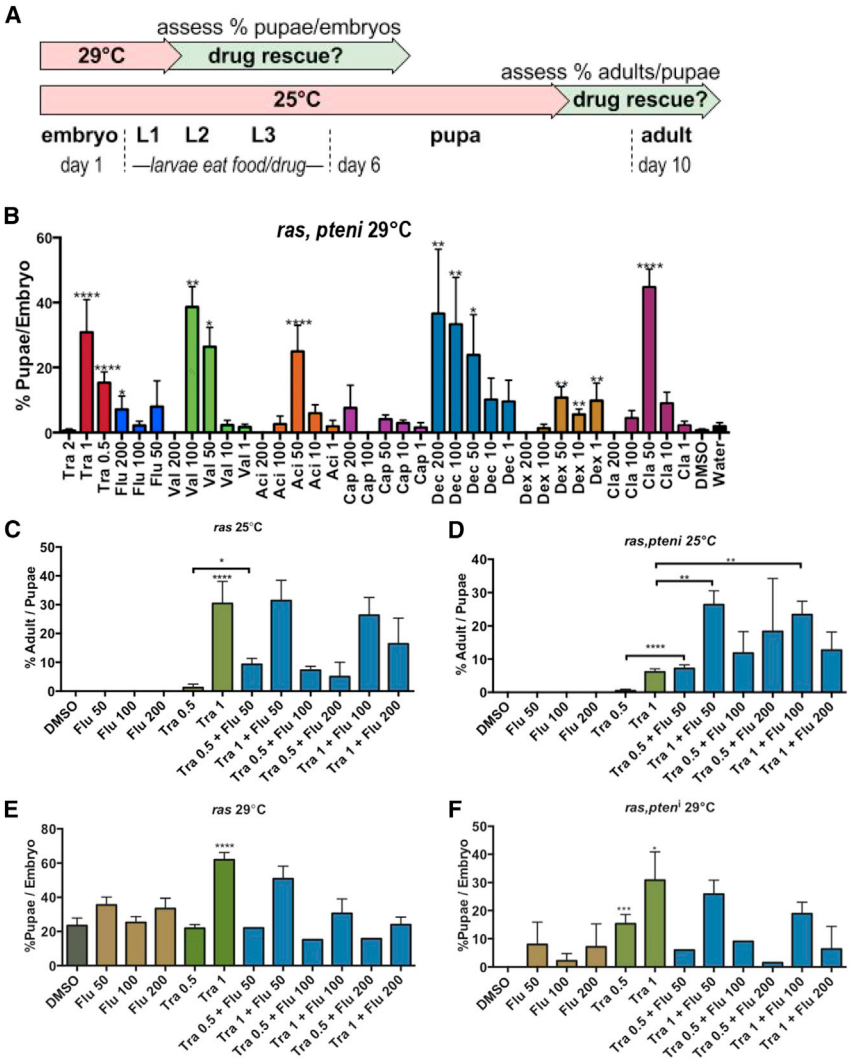

Figure 2. A Lethality-Based Large-Scale Drug Screen

(A) Flowchart of drug experiments. *btl* > *Ras1* combinations led to early larval lethality at 29°C and late pupal lethality at 25°C; drug efficacy was determined by measuring the ratio of pupae:embryos at 29°C or adults:pupae at 25°C.

(B) Nine positive hits from an FDA library screen were tested in larger-scale format (*p ≤ 0.05, ** p ≤ 0.01, *** p ≤ 0.01, and **** p ≤ 0.0001). All drug concentrations are μM. Aci, aciclovir; Cap, capecitabine; Cla, cladribine; Dec, decitabine; Dex, dexrazoxane; Flu, fluvastatin; Tra, trametinib; Val, valaciclovir.

(C) One micromolar trametinib rescued *btl* > *Ras1* pupal lethality (p ≤ 0.0001) at 25°C. Fifty micromolar fluvastatin + 0.5 μM trametinib rescued more fully than 0.5 μM trametinib alone (p ≤ 0.05).

(D) One micromolar trametinib rescued *blt* > *Ras1*,*PTEN* larval lethality (p ≤ 0.0001) at 25°C. Fluvastatin synergized with trametinib at select concentrations.

(E) One micromolar trametinib rescued *btl* > *Ras1*,*PTENi* pupal lethality (p ≤ 0.0001) at 29°C; fluvastatin failed to improve rescue.

(F) Trametinib at 0.5 μM (p ≤ 0.01) and 1 μM (p ≤ 0.05) rescued *btl* > *Ras1*,*PTENi* larval lethality at 29°C; high levels of fluvastatin failed to improve trametinib-based rescue in experiments presented in (C)–(F), presumably due to toxicity at 200 μM.

Values represent mean ± SEM.

cancer patients. We therefore focused on the targeted therapeutic drugs trametinib and fluvastatin.

Trametinib and Fluvastatin Synergized to Rescue Cancer-like Phenotypes

Combining 50 μM fluvastatin with 0.5 μM trametinib significantly enhanced rescue of pupal lethality for both genotypes (Figures 2C and 2D) compared to oral administration of trametinib alone. Further, combining 50 μM fluvastatin with 1 μM trametinib also significantly enhanced rescue of pupal lethality in *btl* > *Ras1*,*PTENi* (Figure 2D) though not *btl* > *Ras1* (Figure 2C) compared to 1 μM trametinib alone. Combining fluvastatin with trametinib did not enhance rescue of larval lethality for either genotype (Figures 2E and 2F). These data indicate that trametinib is a strong inhibitor of Ras1-based lethality and fluvastatin is a weaker inhibitor. Combining specific concentrations of fluvastatin with trametinib yielded synergistic behavior in promoting adult viability that is more robust in *btl* > *Ras1*,*PTENi* than *btl* > *Ras1* alone. Given the potential clinical relevance of this two drug combination, we further explored their ability to synergize.

In the absence of drug, *btl* > *Ras1*,*PTENi* L3 larvae displayed thickened tracheal tubes and ectopic fine terminal branching (Figure 1C). Oral administration of 1 μM trametinib nearly completely suppressed *btl* > *Ras1*,*PTENi* tracheal phenotypes. Specifically, *btl* > *Ras1*,*PTENi* animals treated with trametinib did not exhibit the increased terminal branching phenotype observed in DMSO-fed control animals nor did tracheal cells display the "bulging" nuclei that contributed to tracheal thickening (Figures 3B, 3C, and S1).

We did not observe overproliferation or multilayering within the majority of the *btl* > *Ras1*,*PTENi* tracheal system. The cells that make up the larval trachea are polyploid (Makino et al., 1938; Makino, 1938; Edgar and Orr-Weaver, 2001) and are thought to be terminally differentiated though recent reports suggest they can divide (Denes et al., 2015; Weaver and Krasnow, 2008). Primary dorsal branches within the L3 larva's second tracheal metamere, however, displayed ectopic cells compared to controls (Figure S2); this region is populated by dividing imaginal tracheoblasts (Guha and Kornberg, 2005). The second tracheal metamere is the source of mitotically active imaginal tracheoblasts (IT) that are used to repopulate the tracheal system during the larval-to-pupal transition. The second tracheal metamere is bound to the larval wing disc via a transverse connective tracheal branch, which also connects the wing disc to a specialized tracheal structure called the "air sac precursor" (ASP). The ASP

Please cite this article in press as: Levine and Cagan, *Drosophila* Lung Cancer Models Identify Trametinib plus Statin as Candidate Therapeutic, Cell Reports (2016), http://dx.doi.org/10.1016/j.celrep.2015.12.105

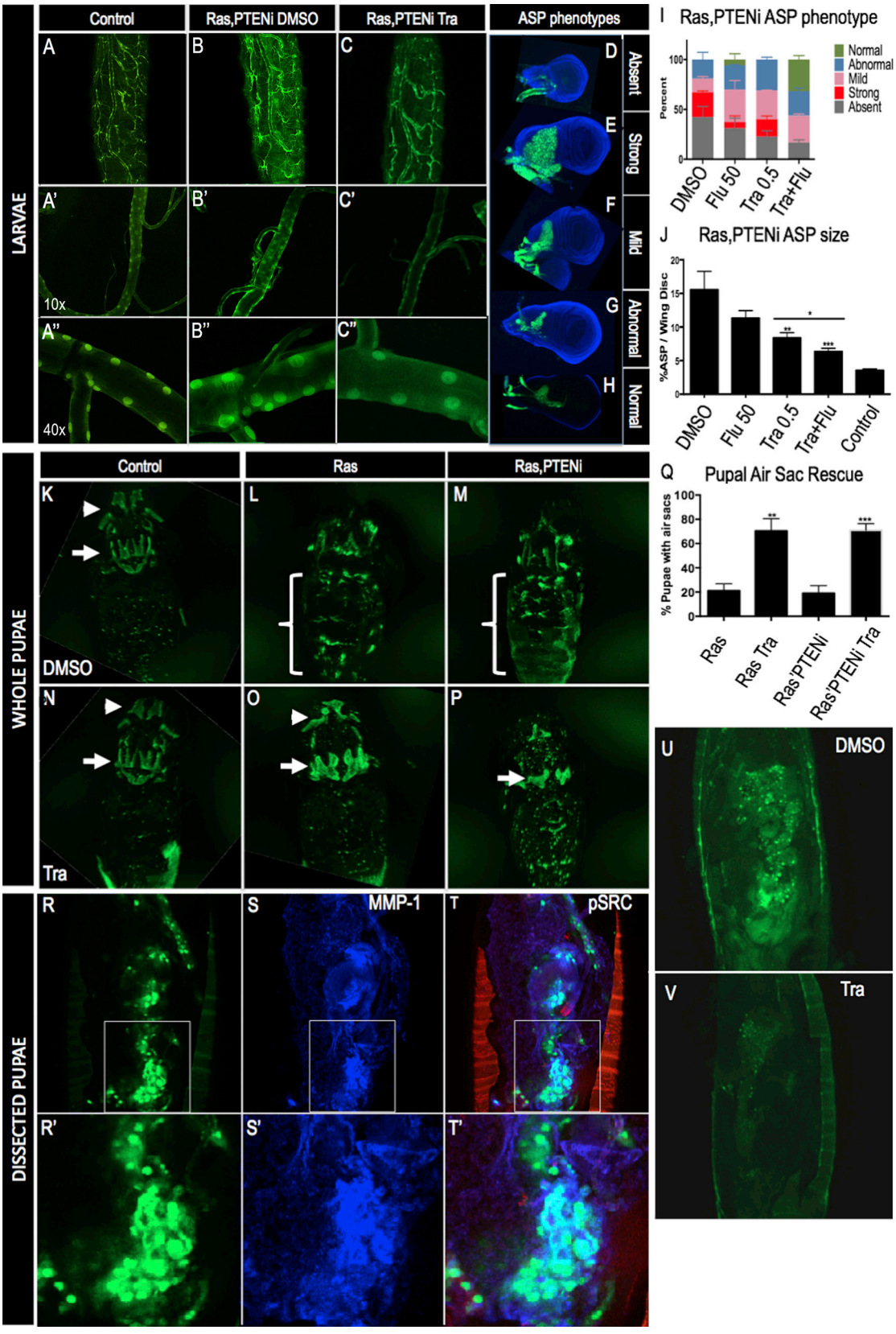

(legend on next page)

is the larval precursor to the large adult dorsal air sacs and provides a readily visualized assay. At the L3 stage of larval development, the ASP forms from a small population of mitotically active cells (Sato and Kornberg, 2002), proliferating and migrating toward a localized signal of FGF in the dorsal notum region of the wing disc (Sato and Kornberg, 2002). During the animal's transition from larva to pupa, the majority of larval tracheal cells will histolyze; the pupal trachea is repopulated from imaginal cells similar to those that form the ASP (Yin and Thummel, 2005).

btl > *Ras1*,*PTENi* animals displayed a range of ASP phenotypes (Figures 3D–3G). Forty-two percent of dissected *btl* > *Ras1*,*PTENi* wing discs lacked ASPs and 19% were small or abnormally shaped (Figure 3G), suggesting that these ASPs failed to form properly. Thirty-nine percent of *btl* > *Ras1*,*PTENi* ASPs were enlarged; some were significantly overgrown and filled the dorsal region of the wing disc whereas others displayed milder overgrowth phenotypes (Figures 3E and 3F). 0.5 μM trametinib reduced the percentage of animals with absent ASPs to 23% compared to 42% in control animals fed DMSO. Fifty micromolar fluvastatin also led to a mild rescue of ASP loss (31%).

Combining trametinib plus fluvastatin decreased the percentage of absent ASPs to 17% (Figure 3I) and greatly increased the percentage of normal ASPs to 32% compared to fluvastatin (6%) or trametinib (0%) alone (Figure 3I). We observed no strongly overgrown ASPs in animals fed the two-drug combination (Figure 3I). Control *btl* > *Ras1*,*PTENi* animals fed DMSO had ASPs that comprised 15% of total wing disc size (Figure 3J). Fluvastatin and trametinib lowered ASP volumes to 11% and 8%, respectively. Combining the two drugs further rescued ASP size to 6%, similar to control levels of 4% (Figure 3J).

The ASP matures into dorsal air sacs that are visible in late pupae within the dorsal thorax (Figure 3K). Air sacs in the head formed from dilations of the larval cervical trachea are also visible (Figure 3K). Most *btl* > *Ras1* and *btl* > *Ras1*,*PTENi* pupae displayed a loss of these air sacs (Figures 3L and 3M), consistent with the absence of ASPs observed in larval stages; overall, only 20% retained intact dorsal air sacs. This number was strongly improved to 75% in trametinib-fed animals (Figures 3O–3Q), consistent with trametinib's rescue of larval ASP loss. We also noted ectopic, GFP-positive tumor-like structures present in the abdominal regions of *btl* > *Ras1* and *btl* > *Ras1*,*PTENi* pupae (Figures 3L and 3M). During metamorphosis, most larval tissue including the tracheal epithelium histolyze and are replaced by imaginal tissue (Djabrayan et al., 2014; Cabernard and Affolter, 2005; Sato and Kornberg, 2002). These GFP-positive abdominal tumor-like foci likely derive from regions that failed to histolyze properly (Figures 3R and 3U); alternatively, they may represent migrating cells from larval tracheal areas such as the ASP, which contains cells that endogenously express MMP-1 and migrate across the wing disc. Trametinib consistently reduced the levels of *btl* > *Ras1*,*PTENi* GFP-positive abdominal foci (Figure 3V; n = 60). Fluvastatin alone had no effect, and combining fluvastatin with trametinib did not lead to further reduction (data not shown), presumably due to the already high level of rescue by trametinib alone (Figure 3Q).

btl > *Ras1*,*PTENi* abdominal "tumors" expressed the cancer biomarker MMP1 (Figure 3S). MMP1 is often associated with metastasis (Kessenbrock et al., 2010), and we used time-lapse movies to determine whether *btl* > *Ras1*,*PTENi* abdominal tumors showed migration. GFP-positive cells were observed to migrate significant distances in *btl* > *Ras1*,*PTENi* pupae (Movie S1); similarly, migrating cells were not observed in controls with the caveat that the tracheal system is dynamically reconstructing at this stage and control pupae did not display GFP at strong enough levels to serve as a fully useful comparison.

Fluvastatin Reduced Trametinib's IC_{50} in Human Lung Cancer Cells

To determine whether they exhibited similar synergy in a standard human lung cancer model, the effects of trametinib and fluvastatin were examined in A549 cells, a human lung adenocarcinoma cell line that contains the activated Ras isoform $KRAS^{G12S}$. Dose-response curves of trametinib (Figure 4A) and fluvastatin (Figure 4A) identified each drug's IC_{50} as 31.68 nM and 5,358 nM, respectively. Trametinib dose-response curves were then repeated with fixed doses of 1,000–4,000 nM

Figure 3. Trametinib and Fluvastatin Rescue Tracheal Defects

(A–A'') *btl* > *control* whole larvae (A) and dissected (A' and A'') trachea.

(B–B'') *btl* > *Ras1*,*PTENi* whole larvae have increased fine tracheal branching (B). Dissected *btl* > *Ras1*,*PTENi* trachea displayed thickened tracheal tubes and enlarged cell nuclei (B' and B'').

(C–C'') One micromolar trametinib rescued *blt* > *Ras1*,*PTENi* ectopic fine tracheal branches, tracheal thickening, and enlarged cell nuclei.

(D–G) *btl* > *Ras1*,*PTENi* exhibited multiple alterations in anterior sac precursor (ASP) development including ASP absence (D), strong overproliferation (E), mild overproliferation (F), and abnormal shape (G).

(H) Representative *btl* > *Ras1*,*PTENi* ASP rescued by 0.5 μM trametinib + 50 μM fluvastatin.

(I) In *btl* > *Ras1*,*PTENi* animals, 0.5 μM trametinib + 50 μM fluvastatin increased percentage of normal ASPs and lowered percentage of absent and strongly overgrown ASP phenotypes compared to either drug alone.

(J) In *btl* > *Ras1*,*PTENi* animals, ASPs comprised 15% of wing disc volume compared to 3% in control ASPs. Fifty micromolar fluvastatin mildly and 0.5 μM trametinib significantly ($p \leq 0.01$) rescued ASP overgrowth. Combining both drugs significantly lowered ASP size compared to trametinib alone (bar; $p \leq 0.05$).

(K) Pupal air sacs in whole pupae were visible in *btl* > *control* animals in the head (arrowhead) and thorax (arrow).

(L and M) *btl* > *Ras1* or *btl* > *Ras1*,*PTENi* animals exhibited loss of pupal air sacs and gain of abdominal tumors (brackets).

(N–P) Compared to *btl* > *control* animals (N), 1 μM trametinib rescued pupal air sacs and inhibited abdominal tumors in *btl* > *Ras1* (O) and *btl* > *Ras1*,*PTENi* (P) animals.

(Q) Quantification of 1 μM trametinib rescue of *btl* > *Ras1* ($p \leq 0.01$) and *btl* > *Ras1*,*PTENi* ($p \leq 0.001$) tumor formation.

(R–U) Dissected *btl* > *Ras1*,*PTENi* pupae had large GFP-positive abdominal tumors (R and U) that were MMP1 positive (S). Phosphorylated SRC outlined the pupal casing (T).

(V) One micromolar trametinib consistently rescued formation of pupal abdominal tumors (n = 60).

All experiments were performed at 25°C except ASP phenotyping at 27°C. Values represent mean ± SEM.

A

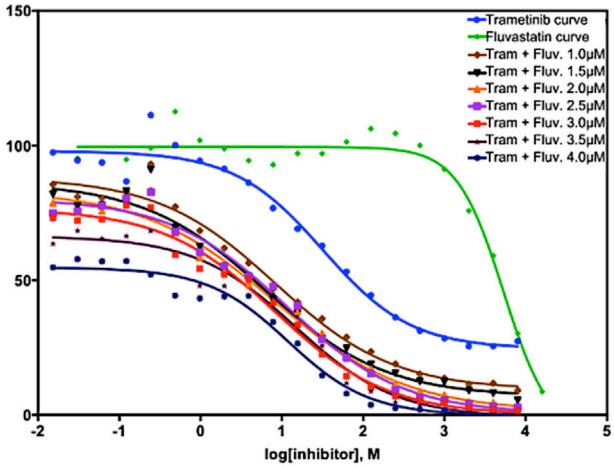

B

Drug	IC50	CI	Result
trametinib curve	31.68		
fluvastatin curve	5358		
tram + fluv. 1000	7.65	0.329	synergy
tram + fluv. 1500	5.87	0.398	synergy
tram + fluv. 2000	8.30	0.552	synergy
tram + fluv. 2500	11.03	0.721	synergy
tram + fluv. 3000	8.19	0.761	synergy
tram + fluv. 3500	13.25	0.997	additive
tram + fluv. 4000	11.73	1.068	additive

Figure 4. Trametinib and Fluvastatin Synergized to Inhibit Growth in A549 Lung Adenocarcinoma Cells

(A) Percent viability of A549 cells determined by MTT assay plotted on a logarithmic molar dose curve scale. Shown are trametinib and fluvastatin single-drug dose curves and fluvastatin dose curve with fixed trametinib dosing.

(B) IC_{50} for fluvastatin, trametinib, and trametinib plus fluvastatin, calculated with Prism software. The combination index (CI) theorem of Chou-Talalay was used to determine synergy versus additive effects. One to three micromolar μM fluvastatin lowered the IC_{50} of trametinib in a synergistic manner.

fluvastatin, below its IC_{50} of 5,358 nM (Figure 4A). Combining fluvastatin with trametinib consistently lowered trametinib's IC_{50} (Figure 4B). Using the Chou-Talalay method to calculate combination index (see Experimental Procedures), we determined that lower doses of fluvastatin (1,000–3,000 nM) exhibited statistical synergy with trametinib (Figure 4B). With these data validating the drug combination across platforms, we next explored their mechanisms of action in a whole-animal setting.

Inhibition of HMG-CoA Reductase and Protein Prenylation Rescued Ras1-Driven Lethality

Fluvastatin is a member of a large family of "statin" drugs that inhibit HMG-CoA reductase, an activity that has proven useful clinically for lowering cholesterol (Figure 5A). Two additional statins, atorvastatin and simvastatin, rescued larval lethality of *btl* > *Ras1* at 29°C at levels comparable to fluvastatin (Figure 5B). Most invertebrates including *Drosophila* do not synthesize cholesterol. They rely on dietary sources of cholesterol, indicating that the cholesterol-lowering action of statins is not their mechanism of action. Another important function of the HMG-CoA reductase pathway is to synthesize the isoprenoid chains geranylgeranyl pyrophosphate and farnesyl pyrophosphate (Figure 5A). These are substrates that are added post-translationally to a variety of proteins—including small GTPases such as Ras—in a process known as prenylation. Prenylation facilitates attachment to the cell membrane and activation of proteins including Ras. We blocked prenylation in *btl* > *Ras1* and *btl* > *Ras1*,*PTENi* flies with oral administration of a geranylgeranyl transferase inhibitor (GGTI) and a farnesyl transferase inhibitor (FTI). The GGTI significantly rescued larval lethality of both *btl* > *Ras1* and *btl* > *Ras1*,*PTENi* at 29°C (Figures 5C and 5D) similar to fluvastatin and showed synergy with trametinib (Figures 5E and 5F). FTI had no effect (Figures 5C and 5D). These results are consistent with results observed when combining trametinib and fluvastatin, further supporting the view that fluvastatin rescues lethality by inhibiting production of isoprenoids such as geranylgeranyl downstream of HMGCR.

Both *btl* > *Ras1* and *btl* > *Ras1*,*PTENi* displayed elevated levels of activated, phosphorylated ERK (pERK) on western blots of dissected L3 tracheal tissue, highlighting activation of the Ras signal transduction pathway (Figure 6A). As anticipated, trachea from animals fed 1 μM trametinib had strongly reduced levels of pERK, below DMSO controls (Figure 6C). Phosphorylation of the PI3K pathway effector AKT was strongly elevated in *btl* > *Ras1*,*PTENi*, confirming the pathway is also activated (Figures 6A and 6B). Whereas trametinib had no effect on pAKT, fluvastatin strongly inhibited pAKT elevation in *btl* > *Ras1*,*PTENi* trachea, indicating that it acted on PI3K pathway activity (Figures 6B and 6D); fluvastatin also showed mild rescue of pERK in *btl* > *Ras1*,*PTENi*, but not *btl* > *Ras1* trachea (Figure 6C).

These data suggest that fluvastatin acts to rescue lethality by at least two mechanisms. Its ability to act by inhibiting PI3K signaling is consistent with previous mammalian studies (e.g., Chu et al., 2006; Li and De Souza, 2011; Son et al., 2007). The ability of fluvastatin to also rescue lethality caused by Ras1 alone—which did not show elevated levels of pAKT—indicates that fluvastatin acts through multiple mechanisms; our inhibitor studies indicate that this includes fluvastatin's ability to block protein prenylation.

Fluvastatin Rescued Drug-Mediated Whole-Animal Toxicity

Whereas up to 1 μM trametinib rescued our transgenic models, higher doses led to reduced eclosion (emergence of adults): 2 μM trametinib led to poor survival in both cancer models and controls that we attributed to whole-animal toxicity. However, combining 50 μM fluvastatin with 2 μM trametinib still led to rescue of *btl* > *Ras1*,*PTENi* pupal lethality (Figure 7A). Feeding 2 μM trametinib to non-transgenic (y^-w^-) flies led to a reduced eclosion rate of 23% compared to 86% of control animals fed DMSO, indicating significant whole-animal toxicity. Combining 100 μM fluvastatin with 2 μM trametinib increased eclosion rate to 57% (Figure 7A). These data indicate that a key aspect of fluvastatin's synergy with trametinib is its ability to reduce the latter's whole-body toxicity profile. Surprisingly, fluvastatin

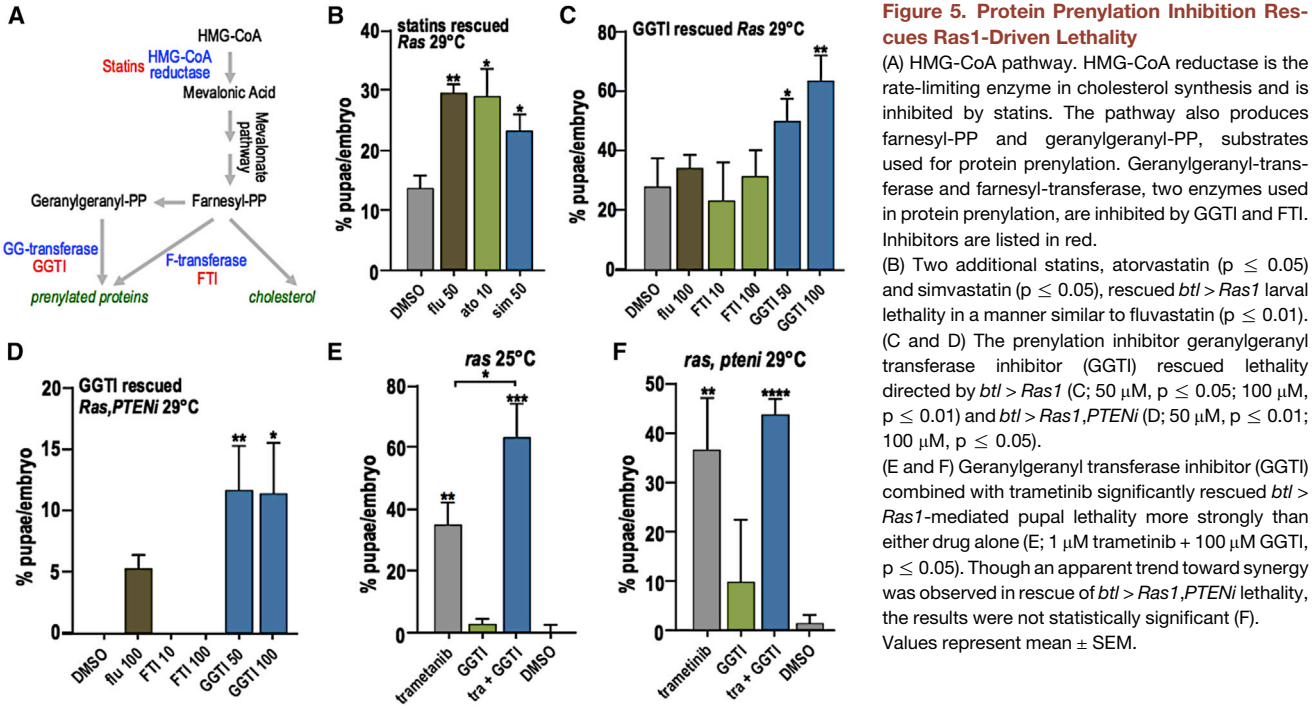

Figure 5. Protein Prenylation Inhibition Rescues Ras1-Driven Lethality

(A) HMG-CoA pathway. HMG-CoA reductase is the rate-limiting enzyme in cholesterol synthesis and is inhibited by statins. The pathway also produces farnesyl-PP and geranylgeranyl-PP, substrates used for protein prenylation. Geranylgeranyl-transferase and farnesyl-transferase, two enzymes used in protein prenylation, are inhibited by GGTI and FTI. Inhibitors are listed in red.

(B) Two additional statins, atorvastatin ($p \leq 0.05$) and simvastatin ($p \leq 0.05$), rescued *btl* > *Ras1* larval lethality in a manner similar to fluvastatin ($p \leq 0.01$).

(C and D) The prenylation inhibitor geranylgeranyl transferase inhibitor (GGTI) rescued lethality directed by *btl* > *Ras1* (C; 50 μM, $p \leq 0.05$; 100 μM, $p \leq 0.01$) and *btl* > *Ras1*,*PTENi* (D; 50 μM, $p \leq 0.01$; 100 μM, $p \leq 0.05$).

(E and F) Geranylgeranyl transferase inhibitor (GGTI) combined with trametinib significantly rescued *btl* > *Ras1*-mediated pupal lethality more strongly than either drug alone (E; 1 μM trametinib + 100 μM GGTI, $p \leq 0.05$). Though an apparent trend toward synergy was observed in rescue of *btl* > *Ras1*,*PTENi* lethality, the results were not statistically significant (F).

Values represent mean ± SEM.

was also able to rescue toxic doses of four other drugs: the proteasome inhibitor bortezomib and three mTOR inhibitors (everolimus, rapamycin, and temsirolimus; Figure 7A).

To understand how fluvastatin reduced drug toxicity, we focused on its activity against HMG-CoA reductase. Reducing enzyme activity by introducing the mutation *hmgcr*^{m102023} or (confirmed hypomorph) *hmgcr*^{01522} (Santos and Lehmann, 2004) protected animals from toxicity due to high levels of trametinib or everolimus (Figures 7B and 7C). Exploring further downstream (Figure 5A), we reduced activity of *Drosophila* orthologs of farnesyl pyrophosphate synthase (FPPS) and geranylgeranyl diphosphate synthase (GGPS) and examined toxic levels of trametinib or everolimus. The FPPS mutant *fpps*^{k03514}, previously demonstrated to decrease levels of Rho prenylation (Cook et al., 2012), was strongly insensitive to trametinib toxicity and mildly insensitive to everolimus toxicity (Figures 7B and 7C). The null allele *ggps1*$^{qm\text{-}L14.4}$ (Santos and Lehmann, 2004) mildly rescued everolimus toxicity (not significant) and had no effect on trametinib toxicity (data not shown). We conclude that, in addition to its anti-tumor effects, fluvastatin can act to reduce whole-body toxicity of specific targeted therapeutics to improve overall therapeutic outcome.

DISCUSSION

A Whole-Animal Drug Screen

We have designed a *Drosophila* transgenic model that provides a whole-animal genetic platform for exploring lung cancer. Pairing targeted activation of Ras1 with loss of PTEN activity (*btl* > *Ras1*,*PTENi*) led to a variety of tracheal defects. Lethality was then used as a quantitative readout to screen a library of 1,192 FDA-approved drugs for the ability to improve overall animal survival. Several hits were known anti-cancer drugs including DNA analogs that presumably act to decrease overproliferation, validating our approach. Our screen also identified a synergistic relationship between the MEK inhibitor trametinib and the HMG-CoA reductase inhibitor fluvastatin.

Our *Drosophila* model is not a precise mimic of lung adenocarcinoma, but it contains important similarities that indicate it can be a useful one. Pairing oncogenic Ras1 with a knockdown of PTEN within the trachea resulted in overproliferation of larval tissue, loss of pupal air sacs, and generation of tumor-like growths in the pupal abdomen. All phenotypes were strongly rescued by trametinib and by trametinib/fluvastatin combinations. Low-dose fluvastatin significantly lowered the IC_{50} of trametinib in inhibiting growth of the Ras1^{G12V}-positive A549 lung adenocarcinoma cell line, demonstrating that fluvastatin acts in part by optimizing trametinib activity within transformed cells. Importantly, the whole-animal aspect of the models also allowed us to distinguish between drug combinations that are therapeutic to the animal as opposed to solely killing cancer cells. This advantage was exploited to determine that—in addition to reducing effects of Ras/PTEN on tracheal integrity—fluvastatin rescued whole-animal toxicity associated with trametinib independent of its effects on transformed cells.

Trametinib/Fluvastatin Synergy

Our results show that, as anticipated, the MEK inhibitor trametinib blocked the rise in pERK associated with overexpression of oncogenic Ras. This is consistent with recent work demonstrating that trametinib acts in *Drosophila* to reduce Ras pathway activity (Slack et al., 2015). Also consistent with

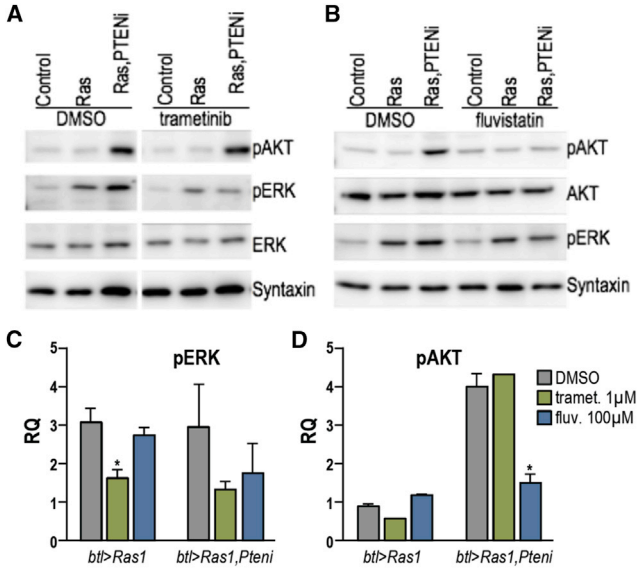

Figure 6. Trametinib Reduced pERK, and Fluvastatin Reduced pAKT

Western blots performed on third instar larval tracheal tissue from *btl > Ras1* or *btl > Ras1,PTENi*.

(A) One micromolar trametinib blocked Ras1-dependent, elevated levels of phosphorylated ERK (pERK) but had no effect on phosphorylated AKT (pAKT).

(B) One hundred micromolar fluvastatin reduced a PTEN1-dependent elevation in pAKT.

(C) Quantification of drug effects on pERK levels, which were strongly reduced by trametinib (Ras1, $p \leq 0.05$; Ras1,PTENi, $p = 0.2513$) and weakly reduced by fluvastatin (Ras1,PTENi, $p = 0.5564$).

(D) Trametinib had no effect on pAKT. Fluvastatin reduced pAKT in *btl > Ras1,PTENi* larvae ($p \leq 0.05$). Values represent mean ± SEM.

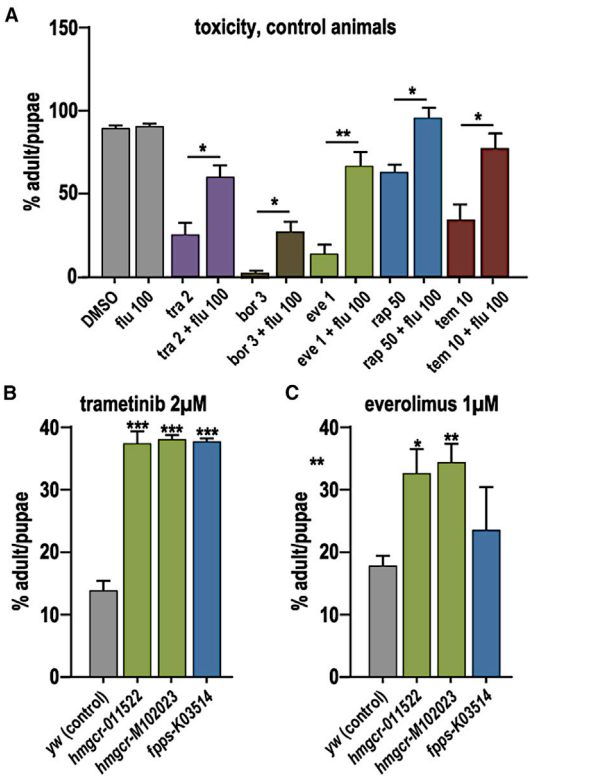

Figure 7. Fluvastatin Rescues Toxicity Caused by Other Drugs

(A) Two micromolar trametinib was toxic to control flies; toxicity was rescued by 50 μM fluvastatin (Flu; $p \leq 0.05$). The proteasome inhibitor bortezomib (bor; $p \leq 0.05$) and three mTOR inhibitors—everolimus (eve; $p \leq 0.01$), rapamycin (rap; $p \leq 0.05$), and temsirolimus (tem; $p \leq 0.05$)—were also toxic at the specified doses (μM). All were partially rescued by 50 μM fluvastatin.

(B and C) Mutant lines of the *Drosophila* homologs of HMG-CoA reductase and farnesyl pyrophosphate synthase were insensitive to trametinib and/or everolimus toxicity.

*$p \leq 0.05$, **$p \leq 0.01$, ***$p \leq 0.01$, and ****$p \leq 0.0001$; values represent mean ± SEM.

mammalian in vitro and in vivo data (Park et al., 2013; Mohammed et al., 2012; Miraglia et al., 2012; Mistafa and Stenius, 2009), statins reduced PI3K pathway activity in *Drosophila* as assessed by reduced phosphorylation of AKT. Though the mechanism underlying statins' role in inhibiting PI3K signaling is not well understood, they may disrupt protein-protein interactions such as KRAS/PI3K (Chen et al., 2013). Fifty micromolar fluvastatin combined with 1 μM trametinib had a significant effect on *btl > Ras1,PTENi* lethality compared to no change in *btl > Ras1* alone (Figures 2C and 2D). This is consistent with fluvastatin's effects on Pi3K signaling. Fluvastatin was not able to consistently enhance trametinib's ability to rescue lethality across all drug concentrations, genotypes, and temperatures. For example, fluvastatin failed to enhance trametinib-based rescue of larval lethality at 29°C (Figures 2E and 2F), possibly reflecting the additional time available to act or differences in larval versus pupal structures.

Statins are traditionally used as cholesterol-lowering drugs. However, *Drosophila* do not synthesize their own cholesterol (Santos and Lehmann, 2004), indicating that this is not the mechanism by which fluvastatin is acting to reduce Ras and PI3K pathway activity. Rather, our data are consistent with the view that the anti-cancer activity of statins is due to their ability to inhibit the synthesis of the downstream isoprenoids farnesyl pyrophosphate (FPP) and geranylgeranyl pyrophosphate (GGPP). Protein prenylation creates a lipidated hydrophobic domain that mediates membrane attachment and protein:protein interactions. Prenylation by FPP and GGPP are critical for post-translational modification of Ras and RhoA proteins, respectively (Mo and Elson, 2004), and inhibiting geranylgeranyl transferase rescued lethality in our *Drosophila* lung cancer models. In mammalian systems, inhibition of Rho protein geranylgeranylation (rather than farnesylation of Ras) is likely an important aspect of the anti-cancer effects of statins (Mo and Elson, 2004; Konstantinopoulos et al., 2007; Wong et al., 2002), consistent with our *Drosophila* data.

Fluvastatin Reduced Whole-Animal Toxicity

A key discovery of this work is the ability of fluvastatin to reduce whole-animal toxicity of multiple targeted drugs independent of its anti-cancer activity. Trametinib is a relatively potent drug including in our cancer models, rescuing lethality at 1 μM food concentration; most effective targeted therapies were optimal within the 100–200 μM range (data not shown). However, trametinib's efficacy was limited by a narrow therapeutic window: 2 μM was toxic to both our cancer model and also wild-type animals.

This is consistent with a well-described toxic profile of trametinib, which includes rashing, gastrointestinal problems, anemia, lymphedema, hypertension, and vascular hemorrhaging, and its use for NSCLC has been limited due to toxicity (Stinchcombe and Johnson, 2014).

Here, we demonstrate that trametinib's toxicity was reduced by fluvastatin. The detailed mechanism behind fluvastatin's ability to rescue trametinib toxicity is not entirely clear. One clue comes from our observation that other targeted therapeutics were similarly rescued by fluvastatin. Fluvastatin rescued the toxicity of the mTOR inhibitors rapamycin, temsirolimus, and everolimus. Inhibition of mTORC1 relieves proteasomal degradation of IRS-1 that results in increased PI3K signaling (Carracedo et al., 2008; O'Reilly et al., 2006; Sun et al., 2005). This suggests that fluvastatin rescues toxicity associated with mTOR inhibition by blocking feedback from activated PI3K signaling, perhaps "re-balancing" Ras/PI3K signaling through the body.

Fluvastatin also rescued the toxicity of the proteasome inhibitor bortezomib. Recent work in our lab suggests that bortezomib can alter PI3K pathway signaling (E. Bangi, personal communication). Other studies have shown that MEK inhibition leads to increased AKT activation by a negative MEK-EGFR-PI3K feedback loop (Faber et al., 2009; Yoon et al., 2009; Hoeflich et al., 2009; Mirzoeva et al., 2009), again consistent with the view that balanced Ras/PI3K signaling is required for whole-body homeostasis. The broad inhibitory nature of statins, due to protein prenylation inhibition, may explain why fluvastatin works well in combination with MEK and PI3K inhibition both directly on cancer cells and in rescuing systemic toxicity. Further studies will be required to determine whether statins show a similar role in improving the therapeutic indices of targeted therapies in patients.

EXPERIMENTAL PROCEDURES

Drosophila Genotypes Used

The following lines were used: y^{-};w^{1118}, *btl-Gal4* (DGRC -109128); $hmgcr^{01152}$ (BL-11522); $hmgcr^{M102023}$ (BL-34720); $fpps^{K03514}$ (BL-10532); and $ggpps^{qm\text{-}L14.4}$ (BL-5828).

In Vitro Assembly of Multi-UAS Vectors

Drosophila genomic DNA from transgenic flies was used to isolate UAS-GFP, UAS-Dicer1, and UAS-Ras1^{G12V}. A vector from the Vienna *Drosophila* Resource Center (VDRC) was used to isolate UAS-PTEN-RNAi (VDRC-35731). The following oligos were used to add SpeI and AvrII sites to the 5′ and 3′ ends, respectively:

5′-cgcactagttccgtggggtttgaattaac-3′
5′-cgccctaggacggcgatatttctgtggac-3′

AvrII was added to the multicloning region of attB-P[acman]-CmR (DGRC-1244). AvrII/SpeI-digested PCR-amplified UAS elements were then ligated into the Pacman vector's AvrII site in the following order: UAS-GFP; UAS-Dicer1; UAS-dRas^{G12V} ; and UAS-PTEN-RNAi in four rounds of cloning. Three vectors (control, Ras1, and Ras1,PTENi) were used to create transgenic lines at the attP 3L-6435776 location (Bloomington no. 24871).

Drug Studies

The Selleck FDA-approved library (catalog no. L1300) was dissolved in DMSO buffer to a 100 mM concentration. A PerkinElmer JANUS automated liquid handler was used to create 1.2 ml 96-well plates (Abgene catalog no. Ab-1068) containing 300 μl fly food and 0.3 μl drug per well. Drug was added to molten (~50°C)-enriched fly food and then left to solidify at room temperature to yield 96-well plates of food with 100 μM drug and a DMSO concentration of 0.1%. *btl* > *Ras1,PTENi* embryos were suspended in a solution of 10% glycerol, 1% BSA, and 0.1% Tween-20. Five to ten microliters of this slurry was added to each well at a concentration of ~20 embryos. Ninety-six-well plates covered with a breathable membrane (Sigma catalog no. Z763624) were placed at 29°C and were scored for the presence of pupae. Positive hits were examined by allowing flies of the indicated genotype to lay 30–60 embryos in 12 × 75 mm, 5 ml test tubes (Sarstedt catalog no. B00471) containing 1 ml of food/drug at the indicated temperature. All inhibitors were from Selleck except the farnesyltransferase inhibitor (Enzo catalog no. G242) and geranylgeranyltransferase inhibitor (Sigma catalog no. G5169).

Histology

For larval trachea and ASP analysis, third-instar trachea or wing discs were fixed in 4% paraformaldehyde. For whole-larvae air sac analysis, late stage pupae (~48 hr after pupae formation [APF]) were collected and the pupal casing was removed prior to imaging. For dissected pupal immunohistochemistry, pupae (~48 hr APF) were frozen in dry ice and then bisected along the anterior-posterior axis, fixed in 4% paraformaldehyde, blocked in 5% BSA PBS-Triton 0.3%. Antibodies used were directed against MMP1 (Developmental Studies Hybridoma Bank catalog no. 3B8D12) and phosphorylated SRC (Invitrogen catalog no. 44660G). Alexa Fluor secondary antibodies were used. Confocal imaging used a Leica DM5500 Q microscope, and image analysis was performed using Adobe Photoshop. ASP and wing disc size were measured by pixel counts using Photoshop histogram.

Western Blots

Trachea from 60 third-instar larvae were dissolved in lysis buffer (50 mM Tris, 150 mM NaCl, 1% Triton X-100, and 1 mM EDTA) supplemented with protease-inhibitor cocktail and phosphatase-inhibitor cocktail (Sigma). Total protein was quantified using Bio-Rad protein assay. Samples were boiled, resolved on SDS-PAGE, and transferred by standard protocols. Antibodies used were from Cell Signaling Technology except ERK (a gift from L. Zipursky) and syntaxin (DSHB). ImageJ software was used for quantification.

MTT Assays using A549 Cancer Line

A549 cell line was cultured in DMEM buffer supplemented with 10% BSA and a penicillin and streptomycin antibiotics mix. Cells were grown in 75 cm^2 sterile polystyrene culture flasks to 80% confluency, trypsinized, and re-seeded in equal aliquots into 96-well plates. After 2 days and ~50 confluency, media was removed and replaced with DMSO or drug-containing media. Cells were allowed to grow for another 6 days, after which the thiazolyl blue tetrazolium bromide (MTT) assay was performed. Cell media was removed and replaced with MTT-containing media (1 mg ml^{-1} final concentration), and cells were allowed to grow at 37°C for another 3.5 hr. MTT media was removed and MTT precipitate dissolved in 4 mM HCl, 0.1% NP40 in isopropanol, solvent by shaking for 1 hr. Spectrophotometric readings at 590 nm and 630 nm using a 96-well plate reader were used to establish growth and viability of cells. Each drug dose was tested in quadruplicates and experiments repeated in triplicate.

Combination index (CI) was determined using the formula outlined by the theorem of Chou-Talalay: CI = ([Tra]c/[Tra]) + ([Flu]c/[Flu]) + ([Tra]c × [Flu]c/[Tra] × [Flu]).

[Tra] and [Flu] are IC_{50} values of the drugs alone; [Tra]c and [Flu]c are IC_{50} values of the drugs in combination. CI values were used to determine synergy (CI < 0.9), additivity (0.9 < CI < 1.1), and antagonism (CI > 1.1) of the drug combinations tested (Chou and Talalay, 1983; Chou, 2010).

Time-Lapse Pupal Movies

Late-stage (>48 hr APF) pupae were selected, placed on a microscope slide, and imaged with a Leica DM5500 Q microscope. Sixty-millisecond exposures were taken every 7 min. Movie shown is 60 frames (7 hr).

SUPPLEMENTAL INFORMATION

Supplemental Information includes two figures and one movie and can be found with this article online at http://dx.doi.org/10.1016/j.celrep.2015.12.105.

Please cite this article in press as: Levine and Cagan, *Drosophila* Lung Cancer Models Identify Trametinib plus Statin as Candidate Therapeutic, Cell Reports (2016), http://dx.doi.org/10.1016/j.celrep.2015.12.105

AUTHOR CONTRIBUTIONS

Conceptualization, Methodology, and Writing, B.D.L. and R.L.C; Investigation, B.D.L.; Funding Acquisition and Supervision, R.L.C.

ACKNOWLEDGMENTS

We thank members of the R.L.C. laboratory for technical assistance and for helpful discussions. We thank Vienna Drosophila Resource Center and the Bloomington Drosophila Stock Center for *Drosophila* reagents. Microscopy was performed in part at the Microscopy Shared Resource Facility at the Icahn School of Medicine at Mount Sinai. This research was supported by NIH grants R01-CA170495, R01-CA170495, and R01-CA109730; Department of Defense grant W81XWH-15-1-0111; and a grant from the Lung Cancer Research Foundation.

Received: August 17, 2015
Revised: October 26, 2015
Accepted: December 30, 2015
Published: January 28, 2016

REFERENCES

Andrew, D.J., and Ewald, A.J. (2010). Morphogenesis of epithelial tubes: Insights into tube formation, elongation, and elaboration. Dev. Biol. *341*, 34–55.

Behr, M. (2010). Molecular aspects of respiratory and vascular tube development. Respir. Physiol. Neurobiol. *173* (*August, Suppl*), S33–S36.

Bellusci, S., Furuta, Y., Rush, M.G., Henderson, R., Winnier, G., and Hogan, B.L. (1997). Involvement of Sonic hedgehog (Shh) in mouse embryonic lung growth and morphogenesis. Development *124*, 53–63.

Cabernard, C., and Affolter, M. (2005). Distinct roles for two receptor tyrosine kinases in epithelial branching morphogenesis in Drosophila. Dev. Cell *9*, 831–842.

Cancer Genome Atlas Research Network (2012). Comprehensive genomic characterization of squamous cell lung cancers. Nature *489*, 519–525.

Carracedo, A., Baselga, J., and Pandolfi, P.P. (2008). Deconstructing feedback-signaling networks to improve anticancer therapy with mTORC1 inhibitors. Cell Cycle *7*, 3805–3809.

Chen, J., Bi, H., Hou, J., Zhang, X., Zhang, C., Yue, L., Wen, X., Liu, D., Shi, H., Yuan, J., et al. (2013). Atorvastatin overcomes gefitinib resistance in KRAS mutant human non-small cell lung carcinoma cells. Cell Death Dis. *4*, e814.

Chou, T.-C. (2010). Drug combination studies and their synergy quantification using the Chou-Talalay method. Cancer Res. *70*, 440–446.

Chou, T.-C., and Talalay, P. (1983). Analysis of combined drug effects: a new look at a very old problem. Trends Pharmacol. Sci. *4*, 450–454.

Chu, G., Jia, R., and Yang, D. (2006). Fluvastatin prevents oxidized low-density lipoprotein-induced injury of renal tubular epithelial cells by inhibiting the phosphatidylinositol 3-kinase/Akt-signaling pathway. J. Nephrol. *19*, 286–295.

Cook, M., Mani, P., Wentzell, J.S., and Kretzschmar, D. (2012). Increased RhoA prenylation in the loechrig (loe) mutant leads to progressive neurodegeneration. PLoS ONE *7*, e44440.

Denes, A.S., Kanca, O., and Affolter, M. (2015). A cellular process that includes asymmetric cytokinesis remodels the dorsal tracheal branches in Drosophila larvae. Development *142*, 1794–1805.

Djabrayan, N.J.-V., Cruz, J., de Miguel, C., Franch-Marro, X., and Casanova, J. (2014). Specification of differentiated adult progenitors via inhibition of endocycle entry in the Drosophila trachea. Cell Rep. *9*, 859–865.

Edgar, B.A., and Orr-Weaver, T.L. (2001). Endoreplication cell cycles: more for less. Cell *105*, 297–306.

Faber, A.C., Li, D., Song, Y., Liang, M.C., Yeap, B.Y., Bronson, R.T., Lifshits, E., Chen, Z., Maira, S.M., García-Echeverría, C., et al. (2009). Differential induction of apoptosis in HER2 and EGFR addicted cancers following PI3K inhibition. Proc. Natl. Acad. Sci. USA *106*, 19503–19508.

Guha, A., and Kornberg, T.B. (2005). Tracheal branch repopulation precedes induction of the Drosophila dorsal air sac primordium. Dev. Biol. *287*, 192–200.

Hoeflich, K.P., O'Brien, C., Boyd, Z., Cavet, G., Guerrero, S., Jung, K., Januario, T., Savage, H., Punnoose, E., Truong, T., et al. (2009). In vivo antitumor activity of MEK and phosphatidylinositol 3-kinase inhibitors in basal-like breast cancer models. Clin. Cancer Res. *15*, 4649–4664.

Kandoth, C., McLellan, M.D., Vandin, F., Ye, K., Niu, B., Lu, C., Xie, M., Zhang, Q., McMichael, J.F., Wyczalkowski, M.A., et al. (2013). Mutational landscape and significance across 12 major cancer types. Nature *502*, 333–339.

Kessenbrock, K., Plaks, V., and Werb, Z. (2010). Matrix metalloproteinases: regulators of the tumor microenvironment. Cell *141*, 52–67.

Konstantinopoulos, P.A., Karamouzis, M.V., and Papavassiliou, A.G. (2007). Post-translational modifications and regulation of the RAS superfamily of GTPases as anticancer targets. Nat. Rev. Drug Discov. *6*, 541–555.

Li, S., and De Souza, P. (2011). Ras isoprenylation and pAkt inhibition by zoledronic acid and fluvastatin enhances paclitaxel activity in T24 bladder cancer cells. Cancers (Basel) *3*, 662–674.

Makino, S. (1938). A morphological study of the nucleus in various kinds of somatic cells of Drosophila virilis. Cytologia *9*, 272–282.

Makino, S., Niiyama, H., and Asana, J.J. (1938). On the supernumerary chromosomes in the mole-cricket Gryllotalpa africana de BEAUVOIS from India (a peliminary report). Jpn. J. Genet. *14*, 272–277.

Miraglia, E., Högberg, J., and Stenius, U. (2012). Statins exhibit anticancer effects through modifications of the pAkt signaling pathway. Int. J. Oncol. *40*, 867–875.

Mirzoeva, O.K., Das, D., Heiser, L.M., Bhattacharya, S., Siwak, D., Gendelman, R., Bayani, N., Wang, N.J., Neve, R.M., Guan, Y., et al. (2009). Basal subtype and MAPK/ERK kinase (MEK)-phosphoinositide 3-kinase feedback signaling determine susceptibility of breast cancer cells to MEK inhibition. Cancer Res. *69*, 565–572.

Mistafa, O., and Stenius, U. (2009). Statins inhibit Akt/PKB signaling via P2X7 receptor in pancreatic cancer cells. Biochem. Pharmacol. *78*, 1115–1126.

Mo, H., and Elson, C.E. (2004). Studies of the isoprenoid-mediated inhibition of mevalonate synthesis applied to cancer chemotherapy and chemoprevention. Exp. Biol. Med. (Maywood) *229*, 567–585.

Mohammed, A., Qian, L., Janakiram, N.B., Lightfoot, S., Steele, V.E., and Rao, C.V. (2012). Atorvastatin delays progression of pancreatic lesions to carcinoma by regulating PI3/AKT signaling in p48Cre/+ LSL-KrasG12D/+ mice. Int. J. Cancer *131*, 1951–1962.

O'Reilly, K.E., Rojo, F., She, Q.B., Solit, D., Mills, G.B., Smith, D., Lane, H., Hofmann, F., Hicklin, D.J., Ludwig, D.L., et al. (2006). mTOR inhibition induces upstream receptor tyrosine kinase signaling and activates Akt. Cancer Res. *66*, 1500–1508.

Park, W.Y., Miranda, B., Lebeche, D., Hashimoto, G., and Cardoso, W.V. (1998). FGF-10 is a chemotactic factor for distal epithelial buds during lung development. Dev. Biol. *201*, 125–134.

Park, Y.H., Jung, H.H., Ahn, J.S., and Im, Y.-H. (2013). Statin induces inhibition of triple negative breast cancer (TNBC) cells via PI3K pathway. Biochem. Biophys. Res. Commun. *439*, 275–279.

Roeder, T., Isermann, K., Kallsen, K., Uliczka, K., and Wagner, C. (2012). A Drosophila asthma model - what the fly tells us about inflammatory diseases of the lung. Adv. Exp. Med. Biol. *710*, 37–47.

Santos, A.C., and Lehmann, R. (2004). Isoprenoids control germ cell migration downstream of HMGCoA reductase. Dev. Cell *6*, 283–293.

Sato, M., and Kornberg, T.B. (2002). FGF is an essential mitogen and chemoattractant for the air sacs of the drosophila tracheal system. Dev. Cell *3*, 195–207.

Shiga, Y., Tanaka-Matakatsu, M., and Hayashi, S. (1996). A nuclear GFP/β-galactosidase fusion protein as a marker for morphogenesis in living *Drosophila*. Dev. Growth Differ. *38*, 99–106.

Slack, C., Alic, N., Foley, A., Cabecinha, M., Hoddinott, M.P., and Partridge, L. (2015). The Ras-Erk-ETS-signaling pathway is a drug target for longevity. Cell *162*, 72–83.

Son, B.-K., Kozaki, K., Iijima, K., Eto, M., Nakano, T., Akishita, M., and Ouchi, Y. (2007). Gas6/Axl-PI3K/Akt pathway plays a central role in the effect of statins on inorganic phosphate-induced calcification of vascular smooth muscle cells. Eur. J. Pharmacol. *556*, 1–8.

Stinchcombe, T.E., and Johnson, G.L. (2014). MEK inhibition in non-small cell lung cancer. Lung Cancer *86*, 121–125.

Sun, S.Y., Rosenberg, L.M., Wang, X., Zhou, Z., Yue, P., Fu, H., and Khuri, F.R. (2005). Activation of Akt and eIF4E survival pathways by rapamycin-mediated mammalian target of rapamycin inhibition. Cancer Res. *65*, 7052–7058.

Weaver, M., and Krasnow, M.A. (2008). Dual origin of tissue-specific progenitor cells in Drosophila tracheal remodeling. Science *321*, 1496–1499.

Wong, W.W.L., Dimitroulakos, J., Minden, M.D., and Penn, L.Z. (2002). HMG-CoA reductase inhibitors and the malignant cell: the statin family of drugs as triggers of tumor-specific apoptosis. Leukemia *16*, 508–519.

Yin, V.P., and Thummel, C.S. (2005). Mechanisms of steroid-triggered programmed cell death in Drosophila. Semin. Cell Dev. Biol. *16*, 237–243.

Yoon, Y.-K., Kim, H.-P., Han, S.-W., Hur, H.-S., Oh, Y., Im, S.-A., Bang, Y.-J., and Kim, T.-Y. (2009). Combination of EGFR and MEK1/2 inhibitor shows synergistic effects by suppressing EGFR/HER3-dependent AKT activation in human gastric cancer cells. Mol. Cancer Ther. *8*, 2526–2536.